REPORT DOCUMENTATION PAGE

AFRL-SR-AR-TR-03-

0075

1. REPORT DATE (DD-MM-YYYY)	2. REPORT TYPE	3. DATES COVERED (From - To)
28 February 2003	Final Report	12/01/01 - 11/30/02

4. TITLE AND SUBTITLE

Control of Combustion Instabilities by Variation of Liquid Fuel Spray Properties

5a. CONTRACT NUMBER
F49620-02-1-0035

5b. GRANT NUMBER
F49620-02-1-0035

5c. PROGRAM ELEMENT NUMBER

6. AUTHOR(S)

J.-Y.Lee, E. Lubarsky and B.T. Zinn

5d. PROJECT NUMBER

5e. TASK NUMBER

5f. WORK UNIT NUMBER

7. PERFORMING ORGANIZATION NAME(S) AND ADDRESS(ES)

Georgia Tech Research Corporation
Georgia Institute of Technology
Centennial Reasearch Building, Room 246
Atlanta, GA 30332-0420

8. PERFORMING ORGANIZATION REPORT NUMBER

1606U47

9. SPONSORING / MONITORING AGENCY NAME(S) AND ADDRESS(ES)

AFOSR/PK4 NA
USAF, AFRL
AF Office of Scientific Research
801 N. Randolph Street, Room 732
Arlington, VA 22203
Tomphy Harr

10. SPONSOR/MONITOR'S ACRONYM(S)

A. A.

11. SPONSOR/MONITOR'S REPORT NUMBER(S)

12. DISTRIBUTION / AVAILABILITY STATEMENT

Approved for public release - distribution unlimited.

20030326 019

13. SUPPLEMENTARY NOTES

14. ABSTRACT

This paper describes an experimental investigation of "slow" active control of combustion instabilities by changing the liquid fuel spray properties. Such control approach whose characteristic time is generally much longer than that of the period of the unstable oscillations needs "one time" variation of control inputs in response to changes in engine operating conditions. Using two types of fuel injectors that can produce large controllable variation of fuel spray properties, this study examined the dependence of acoustics-combustion process coupling, i.e., the driving of combustion instabilites upon liquid fuel spray droplet size, which affects the characteristic combustion time and, thus, the coupling between the acoustics and the combustion process. It was demonstrated that changing the spray characteristics significantly damps the instabilities. The results of this study strongly suggest that "slow" active control of the fuel spray droplet sizes with advanced injectors in real engines could be used to prevent the onset of detrimental combustion instabilites.

15. SUBJECT TERMS

Combustion Instability and Active Control

16. SECURITY CLASSIFICATION OF:			17. LIMITATION OF ABSTRACT	18. NUMBER OF PAGES	19a. NAME OF RESPONSIBLE PERSON
a. REPORT	b. ABSTRACT	c. THIS PAGE			Dr. Ben T. Zinn
Final Report			UL	16	19b. TELEPHONE NUMBER (include area code) 404-894-3033

FINAL PERFORMANCE REPORT

FOR PERIOD
DECEMBER 1, 2001 – NOVEMBER 30, 2002

AIR FORCE CONTRACT #: F49620-02-1-0035

SUPPRESSION OF COMBUSTION INSTABILITY BY CONTROLLING SPRAY PROPERTIES IN LIQUID-FUELED COMBUSTORS

PREPARED BY

J.-Y. Lee [*], E. Lubarsky[†] and B.T. Zinn [‡]

Aerospace Combustion Laboratory
School of Aerospace Engineering
Georgia Institute of Technology
Atlanta, Georgia 30332-0150

February 28, 2003

---

[*] Ph.D. Student and Graduate Research Assistant
[†] Research Engineer and AIAA Member
[‡] David S. Lewis Jr. Chair, Regents Professor, and AIAA Fellow

ABSTRACT

This paper describes an experimental investigation of "slow" active control of combustion instabilities by changing the liquid fuel spray properties. Such control approach whose characteristic time is generally much longer than that of the period of the unstable oscillations needs "one time" variation of control inputs in response to changes in engine operating conditions. Using two types of fuel injectors that can produce large controllable variation of fuel spray properties, this study examined the dependence of acoustics-combustion process coupling, i.e., the driving of combustion instabilities upon liquid fuel spray droplet size, which affects the characteristic combustion time and, thus, the coupling between the acoustics and the combustion process. It was demonstrated that changing the spray characteristics significantly damps the instabilities. The results of this study strongly suggest that "slow" active control of the fuel spray droplet sizes with advanced injectors in real engines could be used to prevent the onset of detrimental combustion instabilities.

INTRODUCTION

Combustion instabilities have been observed in numerous propulsion systems, gas turbines and industrial burners that burn liquid, gaseous and solid fuels. The large amplitude pressure oscillations that accompany these instabilities excite structural vibrations in the combustor and its supports, and enhance heat transfer to the combustor walls. Individually or together, these processes reduce the combustor lifetime and often lead to catastrophic combustor failure [1]. Therefore, the onset of detrimental combustion instabilities must be prevented or, at least, minimized.

Combustion instabilities generally occur when energy supplied to one or more acoustic modes of the combustor by the combustion process exceeds the damping of these modes by, e.g., acoustic energy radiation through the nozzle and viscous dissipation. Their driving depends upon the feedback-like coupling between the chamber acoustics and combustion processes. These acoustic-mode feedback mechanisms that drive the instabilities can be divided into two categories [2,3]: injection coupled and intrinsic mechanisms. Injection coupled instabilities are determined by periodic variation in the reactant injection rates and spray properties driven by acoustic oscillations in the combustor. On the other hand, the interactions between oscillatory flow and heat release processes play a decisive role on intrinsic mechanism and the oscillations of propellant injection rate are negligibly small in this case. This also occurs in the injection-coupled mechanism.

In many cases the acoustic-coupled combustion instabilities involve large-scale oscillations of the flame front downstream near flameholder. In certain conditions the amplitude of the flow motion becomes so large that the flame front rolls up into periodic discrete vortices that enhance propellant mixing. Consequently, more intense burning takes place and the acoustic fluctuation associated with this process triggers the shedding of a new vortex and, thus, the whole process is repeated periodically [4]. Therefore, the vortices also play an essential role in the mechanism of instability. In order to reduce the likelihood of the combustor becoming unstable, i.e., to prevent injection and/or intrinsic coupling, one must either increase the damping and/or decrease the combustion process driving by whatever means possible.

In practice, efforts to prevent instabilities generally attempt to increase the system's damping by, e.g., the addition of Helmholtz resonators or acoustic liners, and/or reduction of the combustion process driving by modification of the combustion process by, e.g., increasing the pressure drop across fuel injector orifices to reduce the sensitivity of the fuel injection rate to combustor oscillations. Another method that has been used to prevent combustion instabilities involves modification of the combustor geometry by, e.g., welding of baffles to the injector face in order to change its acoustic properties and, thus, prevent the excitation of unstable modes (i.e., those that can couple with the combustion process). Unfortunately, development of these passive control approaches [3,5] is costly and time-consuming, and it is generally effective for a specific combustor design and/or a limited range of operating conditions. Consequently, interest in developing active control systems [6] that could be effectively applied to various combustion systems over wide ranges of operating conditions has increased in recent years.

One of the most promising active control approaches damps combustion instabilities by modulating the fuel injection rate at the frequency of the instability with proper control phase and gain in an effort to produce an "out of phase" heat release with respect to the pressure oscillations [7,8]. This is often referred to as a "fast" active control approach because it "operates" the actuator at the frequency of the instability. Its application in airborne engines would require light, durable and robust fuel injectors capable of continuously modulating the fuel injection rate at high frequency without failure. However, developing such fuel injector actuators (FIA) is currently difficult. Therefore, there is a need for developing alternate,

"slow" active control approaches [9,10] that do not employ continuous, high frequency modulation of the fuel injection rate. In contrast to the "fast" active control, the "slow" active control operates at a rate commensurate with that at which operating conditions change within the combustor. While the former requires continuous modulation of the fuel flow rate, the latter needs infrequent activation of the system in response to changes in engine operating conditions. For example, since the combustion instabilities generally occur when the acoustic time is of the same order of magnitude as the characteristic combustion time, these instabilities could be prevented if the combustion time could be changed (one time) by, e.g., changing the spray properties, to eliminate/weaken the coupling between the combustion and acoustic oscillations that drives the instability.

Considerations of the mechanisms that drive combustion instabilities indicate that the process is controlled by two characteristic times: i.e., the acoustic and combustion times. The acoustic time is the period of unstable acoustic mode and the combustion time in liquid fueled combustors is loosely defined as the time required to burn a fuel droplet of a given size. It generally "consists" of the atomization, vaporization, mixing and chemical kinetic times. The acoustic period is the inverse of the frequency of acoustic mode, which depends on the combustion chamber geometry, boundary conditions and the gas temperature (controlled by the global combustor equivalence ratio). These design parameters and operating conditions are generally controlled by other system performance requirements that cannot be readily modified in an effort to stabilize the combustor. Since the combustion time is generally dominated by the droplet vaporization time and in unstable combustors is of the order of the acoustic time [11,12], it is possible that "slow" active control of the fuel spray droplet properties may change the combustion time and, thus, reduce the driving of the instability by the combustion process, resulting in system stabilization.

As indicated above, the spray droplet sizes and velocities produced by the atomizer play a significant role in driving and damping combustion instabilities. This is because the initial droplet size has a primary effect on the vaporization time that is described as d^2-law even though it is based upon quasi-steady arguments [11]. Furthermore, the time delay between the injection and the combustor location where a given droplet burns and releases its energy depends upon the initial droplet size and velocity, and the oxidizer flow velocity. These arguments are supported by the theoretical indication showing that axial combustion instabilities may be promoted/suppressed if the combustion time is close to an odd/even multiple of the half-period of the acoustic oscillation [13]. These arguments again suggest that a "slow" active controller that modifies the spray droplet properties in response to changes in engine operating conditions (in order to change the characteristic combustion time) could be effectively used to prevent the onset of combustion instabilities.

This paper describes an experimental investigation of the suppression of combustion instabilities by controlling the atomizing properties in liquid-fueled combustors. The main objective of this study was to develop an understanding of the performance of novel "slow" active control approaches that are employed to suppress combustion instabilities in liquid-fueled combustors. Specifically, this experimental study investigated the acoustics-combustion process coupling and, thus, the driving of combustion instabilities upon the fuel spray characteristics, which affects the characteristic combustion time. To attain this goal, two different types of fuel injectors were used: 1) a novel internally mixed liquid fuel injector with a vaporizing element and 2) a proprietary fuel injector (Nanomiser™) developed by MicroCoating Technologies. They differed markedly in the operating mechanisms for producing large controllable variation of fuel spray properties to suppress the instabilities. While the latter controlled the liquid fuel spray properties by varying electric power input into the injector, the former did it by changing the mass flow rate ratio of the atomizing air stream to the liquid fuel into the injector's mixing tube. In a parallel effort, to determine the effect of the proposed control approach at the different frequencies of excited acoustic modes, this study used various combustor lengths that exhibited instabilities in the 250 ~ 600 Hz range.

TEST I (Internally Mixed Liquid Atomizer With a Vaporizer Unit)

This section describes an experimental investigation of "slow" active control of combustion instabilities using an internally mixed liquid atomizer with a vaporizer unit. At this test setup, the supply pressures of both the liquid fuel and the atomizing air were manipulated independently to control the fuel spray properties over a wide range. Additionally the combustor geometry was varied by progressively changing the length of the combustor (primary air intake pipe) and, thus, it allows the study of instabilities at different frequencies.

Experimental Facilities

A schematic diagram of the test facility that was used in this study is shown in Fig. 1. The facility consisted of air and fuel supply systems, a quartz combustor and diagnostic systems, which possessed extensive capabilities for oscillating pressure and reaction rate measurements.

A schematic of the investigated combustor is also shown in Fig. 2. The combustor consisted of a quartz tube and a conical flame holder that incorporated an internally mixed air assisted atomizer and a vaporizer. The quartz tube had a 60 mm inside diameter, a thickness of 2.5 mm, and a length of 260 mm. The flame holder's diameter was 34 mm at the tip and its half angle equaled 60°. The diameter of the vaporizer was 27 mm. In order to control the velocity of fuel droplets, the width of the annular passage between the flame holder and the vaporizer could be varied between 0.5 and 3 mm. In this study, the fixed width of 1 mm was used.

It forms a fuel spray by mixing liquid fuel and secondary (atomizing) air in a liquid/air mixing tube (emulsion tube). The generated spray impinges upon a hot vaporizer plate, on top, as it flows towards the combustor, resulting in partial evaporation of the fuel in the spray. The resulting spray then enters the combustor through the annular passage between the vaporizer plate and the conical flame holder. Combustion occurs when the spray mixes with the primary air stream that enters the combustor through the annular opening between the combustor wall and conical flame holder. By controlling the relative amount of the secondary (atomizing) airflow rate, it is possible to control the spray properties (i.e., fuel droplet size and velocity) and, thus, the combustor stability.

All of the reported tests were performed with liquid n-heptane (C_7H_{16}) supplied from a fuel tank pressurized to 1,000 psi. Airflow was divided into two parts: primary air and secondary air. The former was supplied directly into the combustion region and the latter was used as an atomizing agent in the internally mixed atomizer. The secondary air stream was introduced into the combustor together with fuel spray. Arrangements were made to assure that the overall combustor equivalence ratio was kept constant, i.e., the total airflow rate into the combustor remained fixed as the secondary flow rate was changed to control the spray properties. In addition, the primary air intake pipe length could be continuously varied from 510 mm up to 850 mm by use of a '3-piece telescope'-like design to provide capabilities for changing the frequencies of the natural acoustic modes of the combustor. The unstable combustor pressure oscillations were measured using a piezo-electric pressure sensor (Kistler-211B5) located close to the bottom plate of primary air intake pipe.

The fuel flow rate was kept constant at $m_f = 0.47$ g/sec. The total airflow rate was 17.2 g/sec at 40 °C. This resulted in a constant, overall combustor equivalence ratio of $\phi = 0.41$. The secondary airflow rate was varied between 0.3 g/sec and 1 g/sec. These values were adjusted by controlling the supply pressure at the fuel nozzle in the range of 40 ~ 50 psi and the secondary air supply pressure between 2 and 13 psi.

Results and Discussion

To determine the dependence of the characteristics of the instabilities upon the injector's operating conditions and, thus, spray properties, the dependence of the characteristics of the instability upon the air/fuel mass ratio (AFR) inside the injector's mixing tube was investigated in the 250 ~ 600 Hz frequency range.

Typical dependence of the amplitude and frequency of the instabilities upon the AFR is presented in Fig. 3. The two sets of pressure amplitude spectra were obtained for two different air intake duct lengths of L_d = 520 mm and 840 mm (shown in Fig. 3-a and 3-b, respectively) as the AFR varied from 0.62 to 2.05. The length of a quartz combustor was same in all the experiments (i.e., 260 mm). For the Configuration Number I (L_d = 520 mm), the observed frequency of the pressure oscillations was nearly constant (f = 410 Hz, which corresponds to a 3/4-wave length of the combustor) in the entire range of AFR variation. The amplitude of the peak varied, however, significantly. At the AFR = 0.62 ~ 1.5, the amplitude of the peak did not significantly exceed the background level of the spectra, indicating the presence of low or negligible amplitude instabilities in this range. As the AFR increased from 1.64 to 2.05, the instability amplitude increased, and at AFR = 1.85 and 2.05 a distinctive peak was clearly observed and combustion process could be characterized as unstable. More complicated behavior was demonstrated in the tests with Configuration Number II (L_d = 840 mm). In this case, when the AFR was in the 0.64 ~ 2.05 range, two acoustic modes were observed. As the AFR varied from 0.62 to 1.64, the 3/4-wave mode of 290 Hz was dominant. As the AFR was further increased to the 1.85 ~ 2.05 range, the amplitude of this mode diminished and the 5/4-wave mode of 460 Hz became dominant. The distinctive peaks of the 3/4 or 5/4-wave modes were observed in the entire investigated range of AFR variation from 0.62 to 2.05.

Variations of the frequency and amplitude of the two main acoustic modes (3/4 and 5/4-wave) of the investigated combustor for fixed spray properties are shown in Fig. 4. These data were obtained with a

constant AFR = 2.05 as the air inlet duct length was gradually reduced from 840 mm to 520 mm. The frequencies of the both acoustic modes varied in accordance with the length of the combustor. The frequency of the 3/4-wave mode increased from 290 Hz to 430 Hz and frequency of the 5/4-wave mode increased from 460 Hz to 600 Hz. As frequency of the peaks changed, their amplitude also changed, clearly indicating the presence of the maximum amplitude value at the specific frequency.

Results similar to that shown in Fig. 3 and 4 are summarized in Fig. 5. Each set of data obtained with a given injector operating conditions was curve fitted in this figure. Such set of data describes measured changes in the amplitude and frequency of the instability resulting from changing the primary air inlet duct length while keeping the AFR in the injector's mixing tube fixed. This result shows that for a given injector operating condition, there exists combustor configuration (and, thus, frequency) at which the amplitude of the instability attains a maximum. The position of this maximum strongly depends on the AFR value, which controls the fuel spray properties. The frequency of the maximum instability magnitude shifted to lower values as the AFR decreased (i.e., as the spray droplets sizes increased). For example, when a fine spray (AFR = 2.05) was produced, the instability was maximized at 425 Hz, and as the spray's droplet sizes increased (AFR = 1.64) the maximum shifted to 340 Hz. With a very coarse spray (AFR = 0.62) the expected frequency of the instability became 250 Hz. Analysis of the data in this figure also shows that it is possible to completely damp an instability by changing the AFR of a given combustor configuration. For example, for a combustor configuration that produced a 400 Hz-instability, decreasing the AFR from 1.85 to 1.64 effectively reduced the amplitude of the instability to almost zero, thus damping the instability (see the arrow "active control" in Fig. 5).

TEST II (Nanomiser™)

This section describes an experimental investigation of "slow" active control of combustion instabilities using a proprietary fuel injector (Nanomiser™). The effect of the spray properties upon combustion instabilities in four different length combustors (and, thus, different acoustic properties) was studied. The size and velocity distributions of the fuel droplets were measured under cold flow conditions using a phase Doppler particle analyzer and the characteristics of these spays were then correlated with the instability characteristics determined by the deconvolution of selected phase-locked CH*-chemiluminescence images and pressure data.

Experimental Facilities

The experimental facility shown in Fig. 6 was used in this study to investigate "slow" control of combustion instabilities. The facility consisted of air and fuel supply systems, a combustor that integrated an atomizer, and diagnostic systems, which possessed extensive capabilities for the spray characterization and flame visualizations in addition to the diagnostic instruments used in the Test I.

A schematic of the investigated combustor is shown in Fig. 7. It consisted of MCT's Nanomiser™, an air supply system, a conical flame holder, and a quartz combustor tube open at its downstream end. The Nanomiser™ can control its spray properties by varying electric power input into the injector. Additional details of this injector are not provided due to proprietary issues. Instead, this paper briefly describes the performance of this atomizer measured in cold flow tests.

Liquid fuel, n-heptane (C_7H_{16}), pressurized to 1,200 psi, was supplied to the Nanomiser™, which was centered in the air supply system at the upstream end of the combustor. The high pressure forced the fuel to move through the capillary tube of the injector that was connected to a power supply. Spray properties were varied by adjusting the power input to the Nanomiser™.

A two-stage fuel/air mixing process was used. One-third of the airflow was directly injected with swirl into the liquid spray through a set of tangentially oriented orifices, and the remaining two-thirds of the air was supplied into the flame region through the annular opening around the periphery of the conical flame holder. The total airflow rate was 15 g/sec at 300 K, and the maximum fuel flow rate was 1 g/s. The use of a quartz combustor tubes allowed optical access to the flame. The tubes inside diameter and thickness were 42 mm and 1.5 mm, respectively, and tests were conducted with combustor lengths of 390, 500, 610 and 720 mm in order to investigate different instability frequencies.

Diagnostic Techniques

1. Phase Doppler Particle Analyzer (PDPA)

In order to determine the relationships between the fuel droplet diameters and velocities, and frequencies of excited instabilities, an Aerometrics Phase Doppler Particle Analyzer (PDPA) system was used in addition to the diagnostic instruments used in the "fast" active control. This system determined the

dependence of the generated spray properties upon the power input to the Nanomiser™. The PDPA used an argon-ion laser that provided a 2-Watt green laser light at a wavelength of 514.5 nm. A transmitting lens with a focal length of 300 mm and a receiving lens with a focal length of 750 mm were used in the optical path of the PDPA. The receiver was oriented at 30 degrees forward scattering position with respect to the transmitter, to gather light scattered by the droplets. The PDPA could measure droplet sizes in the 0.7 μm to 220 μm range. Both the transmitter and the receiver were mounted on a stationary, rigid platform, while the combustor was mounted on a traversing mechanism able to precisely move along three mutually perpendicular coordinates, thus providing the capability to place any point in the spray at the intersection of the laser beams.

2. Pressure Sensor

The unstable combustor pressure oscillations were measured using an air-cooled piezo-electric pressure sensor (Kistler-211B5). It was located close to the flame holder in order to detect the maximum acoustic pressure amplitude since the instabilities excited the quarter-wave mode of the combustor.

3. High-speed Photography

Combustion zone chemiluminescence was measured to determine the temporal and spatial dependence of the unstable combustion processes. This can be done because the intensity of the reaction rate is proportional to the magnitude of the chemiluminescence. The emission spectra of hydrocarbon flames generally consist of several quantum systems of bands that are superimposed on a continuous background. In this study, the characteristics of the combustion process were determined from measurements of CH* radicals radiation from the flame at 431.5 nm [14]

The flame chemiluminescence was acquired by high-speed photography of the combustion zone. This was performed with a Kodak EktaPro Intensified Imager Camera. This camera is capable of operating with up to 12,000 Hz with a controllable shutter speed, with 1/12 of the full resolution (239x192 pixels). Lower frame rate provides higher resolution. For example, the maximum allowable resolution is 239x32 pixels when the frame rate is set as 6,000 Hz. An image is stored as an 8-bit bitmap image, i.e., each pixel has an integer value between 0 and 255. With the fixed resolution of 239x32 pixels, each image was captured using a triggered signal whose frequency was about 10 times higher than the frequency of instability, thus providing about 10 images per period of the oscillations. This system also provides a TTL output signal, whose maximum and minimum equal around 5 and 0 volts when the shutter is open and closed, respectively. Thus, the measured combustor pressure signal was readily synchronized with the instants at which chemiluminescence was measured. The camera recorded the optical emissions of the combustion region after they passed through a narrow band pass interference filter centered at $\lambda = 430 \pm 5$ nm, corresponding to the CH*-chemiluminescence.

4. Deconvolution Methods

The images obtained by the above described procedure represent measured intensities that were integrated along the line-of-sight of the CH*-chemiluminescence. To understand the radial distribution of combustion process heat release, the recorded images had to be deconvoluted. The Abel transform method [15] was used to reconstruct the actual two-dimensional dependence of the reaction rate from the recorded data. For this purpose, the flame image was artificially manipulated to be rotationally symmetric with respect to the centerline of combustor, as averaging the intensities that were in the same axial location and had same radius. The deconvolution process also assumed that the absorption effects were negligible; i.e., none of the light radiation emitted within the solid angle of the collector was absorbed by the surrounding media prior to reaching the detector.

5. Photomultiplier Tube Detector

To confirm the validity of the results obtained by analysis of the high-speed images, the time dependence of the heat released at various axial locations along the flame was determined from measurements of the spatial dependence of CH* radicals ($\lambda = 431.5$ nm) chemiluminescence [14]. This method is based on the existence of proportionality between the intensity of the luminescence and the reaction rate of the combustion process. This was measured using a setup consisting of a Photo Multiplier Tube (PMT), a narrow band pass interference filter centered at wavelength $\lambda = 430 \pm 5$ nm and an appropriate system of lenses and apertures. This system limited the PMT's instantaneous line of sight to a 3 mm thick cross-section of the reaction zone. The PMT setup was mounted on the remotely controlled support system and moved upwards or downwards with a velocity of about 2.5 mm/s along the combustor as it measured the spatial dependence of the CH* chemiluminescence. The phase of the oscillatory CH* chemiluminescence was determined in reference to the measured pressure. The PMT and pressure signals and a signal indicative of the PMT sight position were acquired and sampled by a computerized data acquisition system.

The sampling rate and total scanning time were adjusted to permit accurate FFT analysis of the signals measured along the combustion zone.

Results and Discussion

1. Cold Flow Experiments

This section describes the results of the cold flow tests that characterized the Nanomiser™ sprays. To describe the operating mode of the Nanomiser™, its power input was normalized by the power that completely vaporizes the supplied fuel flow rate. This normalized parameter is described by the following expression:

$$NIP = \frac{AIP}{\dot{m}_f[h_{fg} + C(T_{boil} - T_o)]} \qquad (1)$$

where *NIP* and *AIP* are the normalized and actual injector power input, respectively, m_f is fuel flow rate, h_{fg} is the heat of vaporization, C is specific heat, and T_o and T_{boil} are initial and boiling temperatures of liquid n-heptane, respectively. These cold flow tests were conducted "in the open" by removing the swirler, flame holder and quartz tube; i.e., only the injector was installed on the traverse and no additional air was injected around the injector. Thus, the sprays were generated in different flow environments in the "open" and "confined" tests. However, once the fuel spray was injected into the "confined" configuration (i.e., combustor), it mixed with the swirling airflow whose direction was approximately normal to the spray flow direction. Consequently, the effect of initial velocity of fuel droplets upon the vaporization time (i.e., characteristic combustion time) could be much smaller than that of fuel droplet size. It's also expected that the droplet size distributions near the injector tip in both configurations would be almost identical.

The spray investigated had the appearance of a jet at low NIP values of up to approximately 0.2. Under these conditions, the PDPA could not properly measure droplet diameters because the spray was too dense. On the other hand, for NIP > 0.6, there were not enough droplets in the spray to allow its reliable characterization by the PDPA since a large fraction of the droplets vaporized. Therefore, the cold flow spray characterization could be only performed in the limited NIP range of 0.2~0.6, where the spray was sufficiently dilute to allow the PDPA to measure the droplet diameters with reasonable accuracy. Also, the nearest vertical position (z) from the injector tip where droplet size and velocity measurements were possible was 16 mm due to the PDPA inability to make measurements in dense sprays. Thus, all the measurements were taken across the fuel spray (i.e., the horizontal x-axis along the optical axes of the PDPA transmitter) at z = 16 mm.

Figure 8 shows the dependence of the Sauter mean diameter (SMD, D_{32}) and mean axial velocity upon the normalized injector power input for m_f = 0.75 g/s. These results were obtained by averaging the data measured at the five center points (x = -2, -1, 0, 1, 2 mm), where x = 0 corresponds to the imaginary (because the spray was not exactly symmetric) centerline of the spray. This was done because most of the liquid volume of fuel passed through this narrow region of about 5 mm in diameter. Maximum droplet's diameters were observed near the centerline of spray, and these diameters decreased with distance towards the spray periphery. Maximum velocities were also observed near the centerline and these velocities decreased in the outward direction. Thus, from a practical point of view, the droplet size and velocity measurements taken in this narrow region fully characterized the spray properties. As pointed out earlier, the droplet size for NIP higher than 0.6 could not be measured, and only velocity measurements were possible for these conditions. The dashed curve in Fig. 8 represents a second order extrapolation of the Sauter mean diameter using two measured data points and D_{32}(NIP=1) = 0 because the droplet size should vanish when the NIP ≥ 1. While the mean velocity in Fig. 8 shows a slight, monotonic increase in slope between 28 m/s and 46 m/s, the droplet size monotonically decreased with increased injector power input. These data show that the Nanomiser™ could control the Sauter mean droplet diameter, D_{32} from near 0 up to 150 μm at the given fuel flow rate (m_f = 0.75 g/s).

2. Characterization of Excited Instabilities

This section describes the dependence of the instabilities upon the fuel spray characteristics and acoustic properties of the combustor. Unless otherwise specified, all of the discussed experiments were performed at the fixed equivalence ratio of ϕ = 0.75, with constant m_f = 0.75 g/s. and m_{air} = 15 g/sec. This operating condition generally resulted in both stable and unstable combustion behaviors depending on the injector power.

The dependence of the amplitude and frequency of the instabilities upon the NIP is presented in Fig. 9. The four sets of rms pressure amplitude spectra were obtained in the four different combustor lengths of 390, 500, 610 and 720 mm (shown in Fig. 9-a, 9-b, 9-c and 9-d, respectively) as the NIP varied from 0 to

0.9. The observed frequency of the pressure oscillations was nearly constant for each combustor length over the entire NIP range. These frequencies approximately equaled 523, 430, 350 and 315 Hz, which correspond to a quarter wave mode of the given combustor length. However, Fig. 9 shows that the amplitude of the instability significantly changed as the NIP was varied.

For L = 390 mm (see Fig. 9-a), the combustor was stable when NIP < 0.45. The combustor became unstable as the NIP increased beyond this level attaining a maximum instability amplitude of 0.78 at NIP = 0.61. Figures 9-b and 9-c show that the 500 mm and 610 mm combustors exhibited similar behavior. These combustors exhibited various levels of the instabilities at very low NIP. As the NIP was increased, the amplitude of the instabilities decreased, attaining minimum values of 0.09 and 0.19 at the NIP of 0.42 and 0.39 for combustor lengths of 500 mm and 610 mm, respectively. As the NIP was further increased, maximum peak of rms pressure increased and reached maximum values of 0.85 and 1.1 at NIP values of 0.58 and 0.5 for L = 500 mm and 610 mm, respectively. These amplitudes diminished thereafter. In tests with the longest combustor (i.e., L = 720 mm, see Fig. 9-d), the trend was similar to that exhibited by 500 mm and 610 mm combustors. In this case, however, the maximum amplitude did not significantly exceed the background level of the spectra over the entire NIP conditions (note that the scale of pressure amplitude used in Fig. 9-d is 1/10 of that used in the other three plots in Fig. 9), indicating the presence of low or negligible amplitude instabilities in this combustor and, thus, its stable operation regardless of the magnitude of the NIP. These results suggest that for fuel droplets Sauter mean diameters D_{32} between 10 μm and 150 μm and combustor frequencies around either 315 Hz (1/4–wave mode) or 950 Hz (3/4-wave mode), coupling between heat release and acoustic oscillations that drives instabilities is not likely to occur due to the "incompatibility" between the corresponding combustion time and acoustic times.

Figure 10 shows the dependence of the peak-to-peak pressure amplitude upon the fuel droplet mean diameter instead of the NIP. This figure effectively summarizes the pressure spectra data presented in Fig. 9. The "conversion" from NIP to D_{32} was accomplished using the results in Fig. 8. It shows that the maxima and minima of the amplitudes of the instabilities were associated with certain droplet sizes. They were maximized at D_{32} = 32, 40, 62 and 68 μm, and minimized at D_{32} = 86, 90, 104 and 130 μm for combustor lengths of 390, 500, 610 and 720 mm, respectively, even though the amplitudes of the oscillations in the longest combustor (i.e., L = 720 mm) were always small. For example, for a combustor length of 500 mm that produced a 430 Hz-instability, decreasing the NIP, which corresponds to increasing D_{32} from 40 μm to 90 μm, dramatically reduced the amplitude of the instability by almost 90%, indicating that in this case the "slow" active control essentially damped the instability. This result clearly shows that combustion instabilities could be controlled by "slow" active control of the fuel spray properties and that changing the spray droplet sizes could be used to attain effective control of instabilities.

Finally, the relationship between the combustion zone (or flame) structure and observed instabilities was also studied. Figure 11 presents selected deconvolution images of the flames obtained during the most unstable and stable operations of the 500 mm long combustor using high-speed photography with a narrow band pass interference filter centered at λ = 430±5 nm, corresponding to the CH*-chemiluminescence. Each window size is 42x120 mm, with the bottom of the window corresponding to the flame holder location. Each image was provided by 32x92 pixels. The number of each picture corresponds to a specific phase during the cycle. These phases were equally spaced and synchronized with the pressure signals. For convenience, the reference pressure signal shown in this figure was "idealized" to appear a sinusoidal.

To understand the spatial distribution of combustion process heat release, the recorded line-of-sight images were deconvoluted. The line-of-sight images were taken at a frequency about 10 times higher than the frequency of instability and each image was averaged by four pictures at the same phase before deconvolution. The Abel transform [15] was used to reconstruct the actual two-dimensional dependence of the reaction rate from the recorded data. For this purpose, the flame image was artificially manipulated to be rotationally symmetric with respect to the centerline of combustor, as averaging the intensities that were in the same axial location and had same radius. The deconvolution process also assumed that the absorption effects were negligible; i.e., none of the light radiation emitted within the solid angle of the collector was absorbed by the surrounding media prior to reaching the detector. The noise around the centerline is typically amplified in the Abel deconvolution procedure because the sensitivity to noise increases due to the decreased volume contributing to the signal [16,17]. Therefore, the intensities of one vertical set of pixels closest to the centerline were smoothened by interpolation with the adjacent two outward pixels.

It is noteworthy that vortex structures were clearly visible in the deconvoluted images. Under unstable operations (see Fig. 11-a), the strong heat release was observed midway between the centerline and the wall at a location around 20 mm downstream from the flame holder and was in phase with the pressure oscillations. This suggests that a large portion of fuel burned at the instance of maximum pressure in this

region, which corresponds to the location where the axial velocity was nearly zero in the near field vortices. In contrast, when the combustor was stable, (see Fig. 11-b) the flame reaction rate was nearly constant during the entire period of oscillations.

The Rayleigh criterion [18] could be used to explain how to change the combustion process heat release to reduce the likelihood of incurring combustion instabilities. Figure 12 describes the spatial dependence of the local Rayleigh index along the 500 mm long combustor centerline plane. In this case, the mathematical representation of the driving by the combustion process is given by the following expression:

$$G = \frac{1}{T}\int_T \int_L \int_R 2\pi r p'(r,z,t)q'(r,z,t)drdzdt \qquad (2)$$

where p', q', T, L and R are the combustor pressure and heat release oscillations, oscillation period, and combustor length and radius, respectively. Thus, the local Rayleigh index along the centerline plane was obtained by summing (which in this case corresponds to averaging) the values of $p'(r,z,t)q'(r,z,t) \approx p'(t)q'(r,z,t)$ at each of the 10 sequential pictures in Fig. 12-a and 12-b over one period of the oscillations. The white background in this figure represents the neutral regions due to the negligible oscillating heat release amplitude. During unstable operation, the Rayleigh index was positive over the entire combustion region when the NIP > 0.6 and, which must have been the cause of the strong instability. It should be noted that in this case particularly strong driving occurred near the zero axial velocity locations of the vortices. On the other hand, the Rayleigh index was positive in some flame regions and negative in others during the stable operation, and the magnitudes of the Rayleigh index were relatively low due to the small magnitude of the pressure oscillation $p'(t)$. Those regions alternately drove and damped the instability, thus preventing the driving of a strong instability.

To demonstrate the "consistency" of the results obtained by the high-speed camera and deconvolution techniques, it was also compared the flame characteristics determined by the high-speed camera (HSC) and the PMT detector, see Fig. 13. The HSC results were "converted" to describe a one-dimensional distribution of heat release along the mean flow direction by weighting the annular volume occupied by each pixel in Fig. 12. In the PMT measurements, each set of CH*-emissions data was divided into 50-60 spatial segments and the data from each segment was analyzed by FFT to determine the amplitude and phase of the CH*-emissions in this segment. Figure 13-a shows that both diagnostic methods provide roughly the same heat release distribution. The slight difference in the magnitudes provided by the two methods at each location can be attributed to the fact that both sets of data were not measured at the same instance due to their different total sampling time requirements.

Figure 13-b shows the phase distribution obtained by the PMT. It shows that the phase between the heat release and pressure oscillations experienced small variations of about zero degrees during the unstable operating condition. On the other hand, the phase gradually increased from 0 to nearly 360 degrees along the reaction zone during stable operation. Figure 13-c presents the spatial dependence of local Rayleigh index. The PMT results were obtained by calculating the product of: 1) the amplitude of measured combustor pressures, 2) the amplitude of the oscillating heat release presented in Fig. 13-a, and 3) the cosine of the phase between these amplitude, given in Fig. 13-b, to obtain the quantity, $|p'(t)||q'(x,t)|\cos\theta$. The results show that high driving occurred throughout the combustion region during unstable operation. However, under stable operation, the magnitude of local Rayleigh index was relatively small and the combustion region was effectively divided into regions that alternately drove and damped the instability. These countering effects tend to cancel one another, resulting in practically stable operation. Both diagnostic methods were found to be in fair agreement with each other and they properly revealed the manner in which driving occurs in the studied combustors.

3. Comparison With "Fast" Active Control Result

In order to elucidate how the manners in which the "slow" and "fast" active controls damp combustion instabilities are different, this section compares both control results.

The experimental setup used to investigate "fast" active control was same with that used in the Test II except the type of a fuel injector used, as shown in Fig. 14. Instead of the Nanomiser™, a fuel injector actuator (FIA) was used to modulate the fuel injection rate at the frequency of instability. On the contrary to the open loop, "slow" controls (Test I and II), this test has been conducted in the closed loop, active, "fast" control experiment: i.e., an observer that determined the characteristics of the instability and a controller that generated control phase and gain needed to damp the instabilities under the indicated operating condition.

The FIA consisted of a Terfenol D type magnetostrictive actuator that was connected to a pintle-type injector. The time dependence of the liquid flow rate through the FIA was controlled by a control current to

a coil wound around the actuator. As the control current changes, the coil's magnetic field also changes. This, in turn, changes the length of the magnetostrictive rod (1). As the actuator's length changes, it pushes the pintle (2) against a pressure force exerted by the liquid fuel supplied into the volume (3) between the pintle's conical termination and the FIA's casing. The resulting force imbalance sets the pintle in motion. As the pintle moves backwards, the annular clearance (4) between the two cones opens and allows liquid fuel to flow through the plenum (5) into the wedge shape nozzle (6). The pressure difference across the nozzle (6) changes as the width of the cross sectional area of the annular clearance (4) changes. This pressure difference forces the liquid to move through the nozzle and produce a spray in the combustor.

Figure 15 compares the pressure spectra in the combustor under the same operating conditions with the "fast" active control system (FACS) "on" and "off" for "lean" and "rich" instabilities. The air flow rate was kept at 12 g/s and the global equivalence ratio ϕ was changed by varying the fuel (n-heptane) flow rate. It shows that the FACS that in addition to slightly changing the frequency of the oscillations, the FACS reduced the amplitude of the unstable mode at $\phi = 1.1$ and $\phi = 0.4$ by factors of 8.3 and 3.2, respectively. Figure 16-a shows that the FACS significantly reduced the amplitude of the oscillations all along the combustor when $\phi = 1$ and had little effect on the amplitude distribution when $\phi = 0.45$. Figure 16-b shows that the FACS modified the "nearly flat" phase distributions, which were observed during unstable operation, to "continuously varying" phase distributions similar to those exhibited by "stable" operation in the "slow" active control test (see Fig. 13-b). For example, when $\phi = 1$, the "controlled" phase varied between approximately –50 and 0 degrees along the first 20 mm. of the combustion region. It then gradually increased from 0 to approximately 100 degrees along the section of the reaction zone located between 20 and 60 mm, and it maintained a nearly constant value of 100 degrees along the remainder of the combustion region. It should be pointed that the driving by the combustion process is nearly zero when the phase is near 90 degrees. The comparison presented in Fig. 16-c, which describes the spatial variation of the integrand of the Rayleigh integral, i.e., $dG(x)/dx$ (see Eq. (2)), show that the FACS significantly reduced the magnitude of $dG(x)/dx$ all along the combustion zone when $\phi = 1$ and along part of the combustion region when $\phi = 0.45$.

The presented results show that active modulation of the fuel spray injection rate damped the instability by essentially modifying the spatial dependence of the phase between the heat addition and pressure oscillations. Specifically, the FACS replaced the "nearly flat" phase distribution, observed during unstable operation, by one that gradually varied along the combustion region. This, in turn, reduced the driving of some regions of the combustion zone and produced "negative" driving (i.e., damping) in other regions of combustion zone. It's also noteworthy that the gradually varying phase distribution produced by the FACS was very similar to that observed during the "slow" active control test. Both control approaches localized the driving region by modifying the combustion process heat release to interfere in the primary driving mechanism. Therefore, it was clearly shown that the manners in which both the "fast" and "slow" active controls damp the combustion instabilities are basically same.

CONCLUDING REMARKS

- The effectiveness of "slow" active control of combustion instabilities by modification of the spray characteristics has been demonstrated with two different injectors; i.e., an effervescent type and a proprietary Nanomiser™ injector.
- The dependence of the instabilities upon the fuel spray characteristics and acoustic properties of the combustor were also studied. It was shown that the spray droplet sizes that produce maximum and minimum instability amplitudes shifted to lower values as the frequency of instability increased, as expected.
- Spatial distributions of CH*- chemiluminescence obtained by image deconvolution revealed the presence of vortex-flame interactions during unstable operation that apparently produces strong driving occurs where the mean axial velocity is nearly zero just downstream of the flame holder.
- It was clearly shown that the manners in which both the "fast" and "slow" active controls damp the combustion instabilities are basically same: i.e., in an effort to modify the combustion process heat release that will partially contribute to damping region and interfere with the primary driving mechanism.

REFERENCES

1. F. E. C. Culick and V. Yang, "Overview of Combustion Instabilities in Liquid-Propellant Rocket Engines," *Progress in Astronautics and Aeronautics*, vol. 169, pp. 3-37, 1995.

2. D. K. Huzel and D. H. Huang, *Modern Engineering for Design of Liquid-Propellant Rocket Engines, Progress in Astronautics and Aeronautics*, vol. 147, pp. 127-134, 1992.

3. D. T. Harrje and F. H. Reardon, *Liquid Propellant Rocket Combustion Instability*, NASA SP-194, pp. 385-449, 1972.

4. T. J. Poinsot, A. C. Trouve, D. P. Veynante, S. M. Candel and E. J. Esposito, "Vortex-Driven Acoustically Coupled Combustion Instabilities," *J. Fluid Mech.*, vol. 177, pp.265-292, 1987.

5. K. C. Schadow and E. Gutmark, "Combustion Instability Related to Vortex Shedding in Dump Combustors and Their Passive Control," *Energy Combust. Sci.*, vol.18(2), pp.117-132, 1992.

6. K. R. McManus, T. Poinsot and S. M. Candel, "Review of Active Control of Combustion Instabilities," *Energy Combust. Sci.*, vol. 19(1), pp.1-29, 1993.

7. C. E. Johnson, J.-Y. Lee, Y. Neumeier, E. Lubarsky and B. T. Zinn, "Suppression of Combustion Instabilities in a Liquid Fuel Combustor Using a Fast Adaptive Control Algorithm," AIAA 2000-0476, *38th Aerospace Sciences Meeting and Exhibit*, Reno, NV, Jan. 2000.

8. F. Kappei, J.-Y. Lee, C. E. Johnson, E. Lubarsky, Y. Neumeier and B. T. Zinn, " Investigation of Oscillatory Combustion Processes in Actively Controlled Liquid Fuel Combustor," AIAA 2000-3348, *36th AIAA/ASME/SAE/ASEE Joint Propulsion Conference*, Huntsville, AL, July 2000.

9. J.-Y. Lee, E. Lubarsky, B. T. Zinn, S. D. Sundell, M. Lal and M. Oljaca, "Optical Diagnostics of Oscillatory Combustion Processes Controlled by Modification of Atomizing Properties," AIAA 2002-0192, *40th Aerospace Sciences Meeting and Exhibit*, Reno, NV, Jan. 2002.

10. J.-Y. Lee, A. Kushari, E. Lubarsky, B. T. Zinn, S. Rozenberg and Y. Levy, "Control of Combustion Instabilities and Emissions Using an Internally Mixed Liquid Atomizer With a Vaporizer," AIAA 2002-0617, *40th Aerospace Sciences Meeting and Exhibit*, Reno, NV, Jan. 2002.

11. W. A. Sirignano, *Fluid Dynamics and Transport of Droplets and Sprays*, Cambridge University Press, Cambridge, 1999.

12. A. Duvvur, C. H. Chiang and W. A. Sirignano, "Oscillatory Fuel Droplet Vaporization: Driving Mechanism for Combustion Instability," *J. Propul. Power*, vol. 12(2), pp. 358-365, 1996.

13. A. P. Vasiliev, *Theoretical Background and Design of the Liquid Rocket Engine*, Visshaia Shkola Pub., Moscow, 1967.

14. R. Mavrodineanu and H. Boiteux, *Flame Spectroscopy*, John Wiley & Sons, New York, 1965.

15. J. Tatum and W. Jarowski, "A Solution of Abel's Equation," *J. Quantitative Spectroscopy and Radiative Transfer*, vol. 38, pp. 319-322, 1987.

16. G. Herding, R. Snyder, C. Rolon and S. Candel, "Investigation of Cryogenic Propellant Flames Using Computerized Tomography of Emission Images," *J. Propul. Power*, vol. 14(2), pp. 146-151, 1998.

17. K. K. Venkataraman, L. H. Preston, D. W. Simons, B. J. Lee, J. G. Lee and D. A. Santavicca, "Mechanism of Combustion Instability in a Lean Premixed Dump Combustor," *J. Propul. Power*, vol. 15(6), pp. 909-918, 1999.

18. L. Rayleigh, *The Theory of Sound*, Dover Pub., New York, 1945.

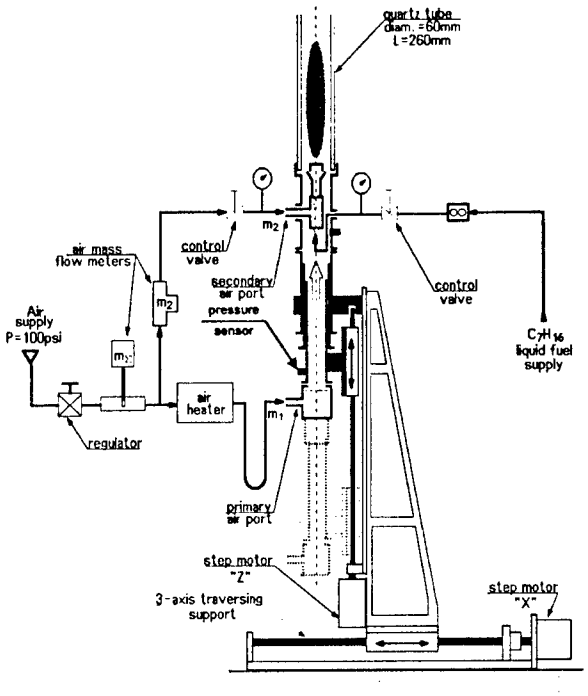

Figure 1. A schematic of the test setup I.

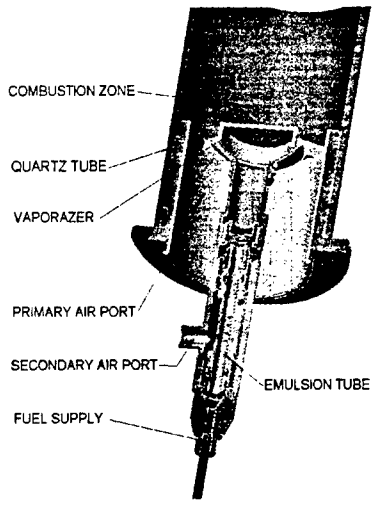

Figure 2. A Schematic of internally mixed injector /vaporizer.

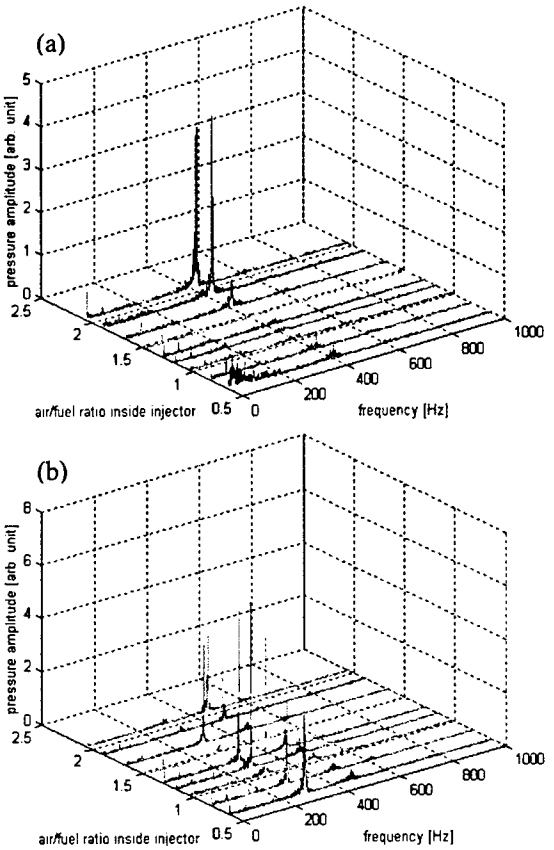

Figure 3. Dependence of the amplitude and frequency of the instability upon the atomizing air/fuel ratio in the injector's mixing tube for two different combustor configurations.
(a) Configuration I: air inlet duct length = 520 mm;
(b) Configuration II: air inlet duct length = 840 mm.

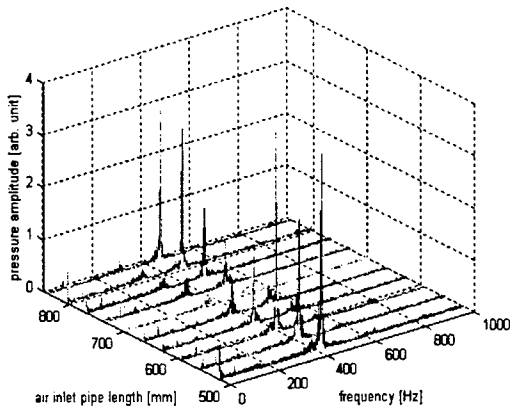

Figure 4. Dependence of the amplitude and frequency of the instability upon the combustor length for the atomizing air/fuel ratio = 2.05.

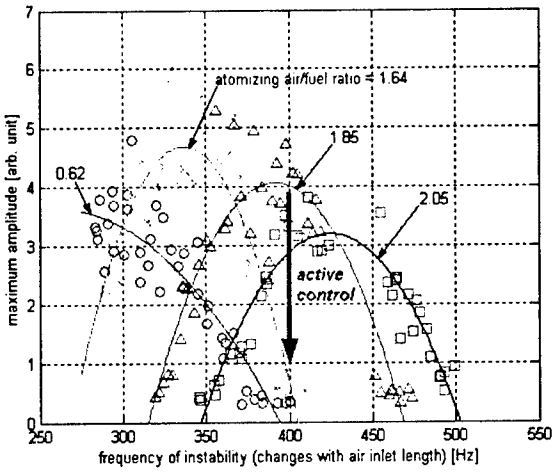

Figure 5. Response of the amplitude and frequency of the instability to changes in the atomizing air/fuel ratio in the injector's mixing tube and air inlet duct length.

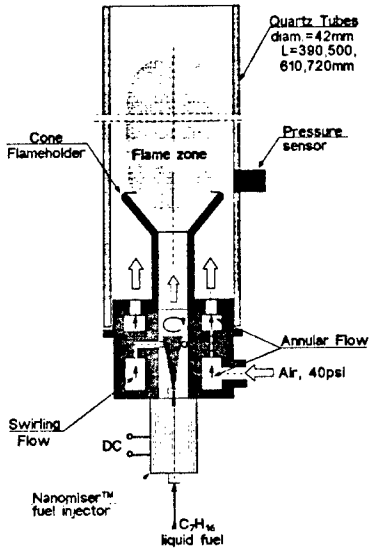

Figure 7. A schematic of the liquid-fueled combustor.

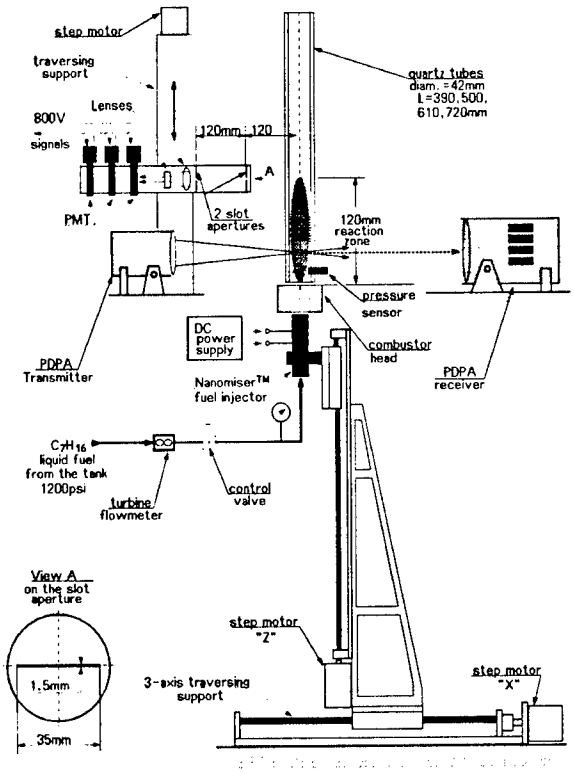

Figure 6. A schematic of the test setup I.

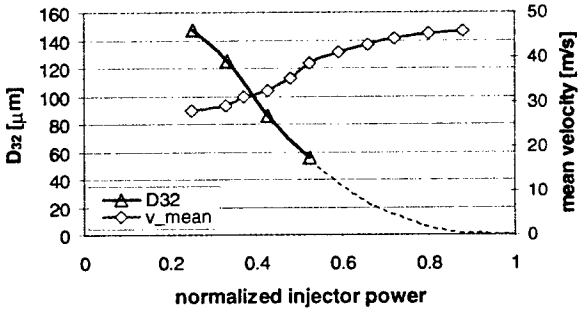

Figure 8. Dependence of the Sauter mean diameter (D_{32}) and mean velocity of the spray droplets upon the normalized injector power input measured 16 mm downstream from the injector tip with m_f = 0.75 g/s.

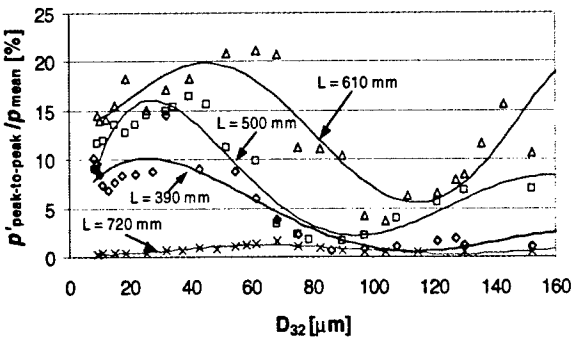

Figure 10. Dependence of the peak-to-peak pressure amplitude upon the fuel droplet mean diameter for the four investigated combustor lengths.

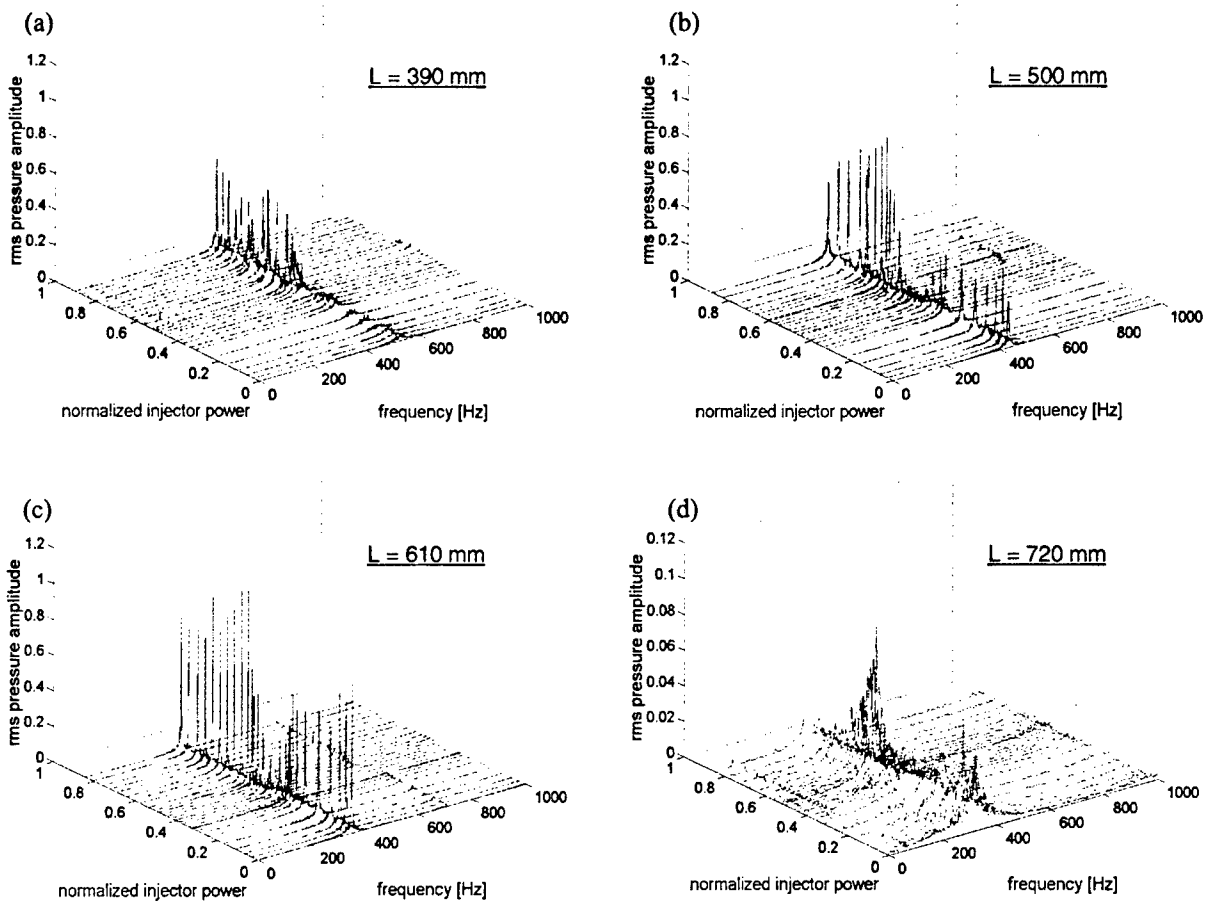

Figure 9. Dependence of the amplitude and frequency of the combustor oscillations upon the injector power input in combustors having the following lengths: (a) L = 390 mm; (b) L = 500 mm; (c) L = 610 mm; (d) L = 720 mm.

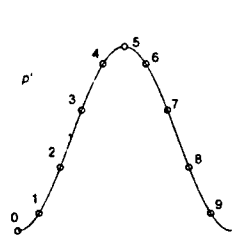

image sequence with respect to the pressure oscillations.

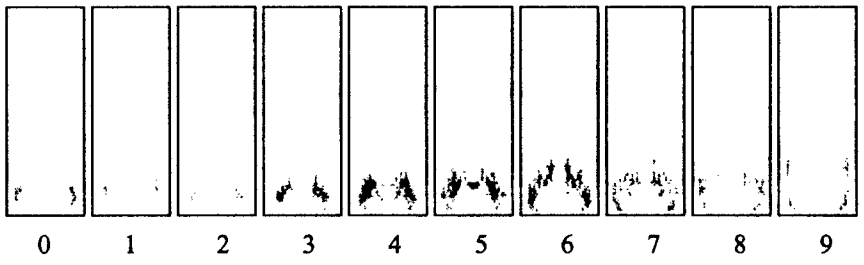

(a) Unstable Operations (NIP=0.58, D_{32}=40 μm)

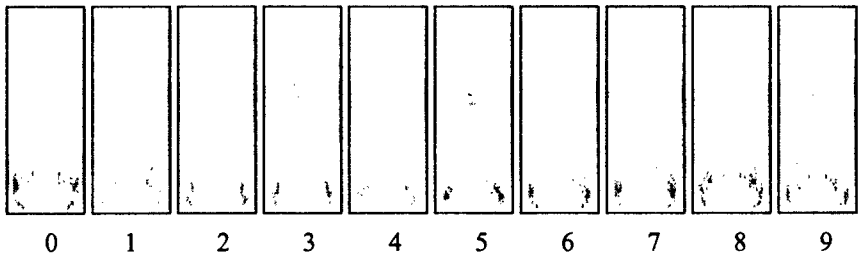

(b) Stable Operations (NIP=0.42, D_{32}=90 μm)

Figure 11. Comparison of the high-speed CH*-chemiluminescence images at the most unstable and stable operations for L = 500 mm.

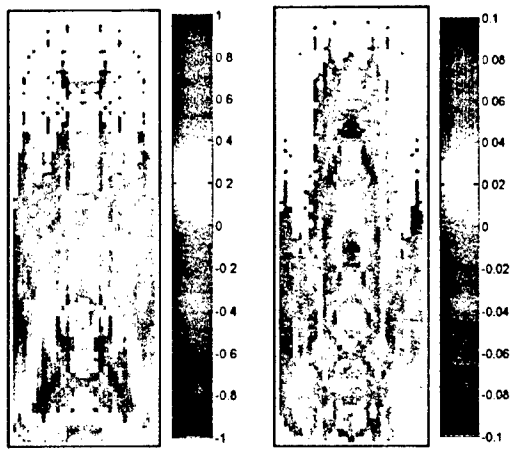

Figure 12. Spatial dependence of local Rayleigh index in the centerline plane of the combustor, L = 500 mm.
(a) Unstable operations; (b) Stable operations.

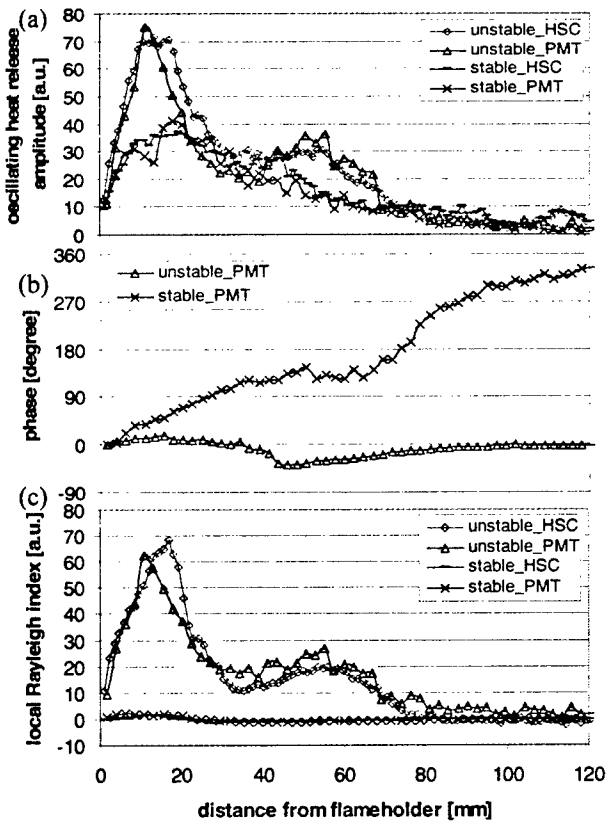

Figure 13. Comparison of the one-dimensional characteristics of the oscillatory combustion processes at the most unstable and stable operations of the combustor, L = 500 mm, obtained from high-speed camera (HSC) visualizations and photomultiplier (PMT) radiation measurements.
(a) Heat release amplitude distribution; (b) Phase distribution; (c) Local Rayleigh index distribution.

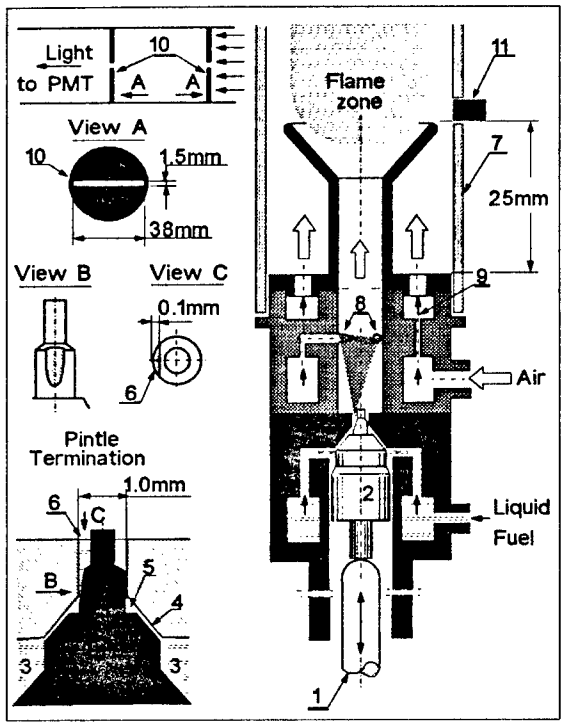

Figure 14. A schematic of the fuel injector actuator (FIA) and combustor head used in "fast" active control test.

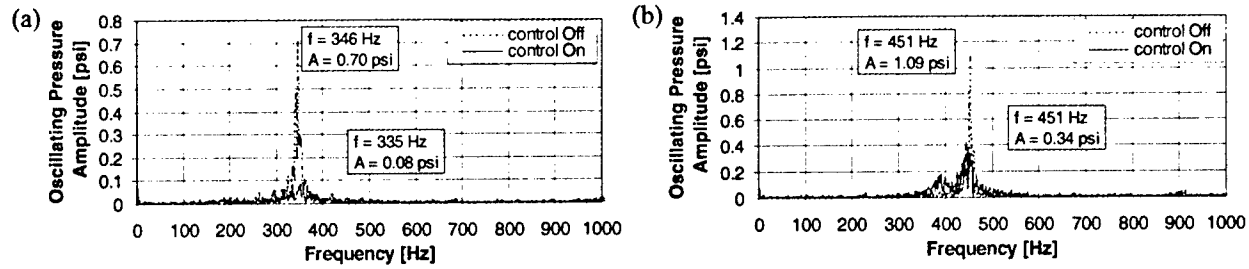

Figure 15. Effect of actively controlled modulation of liquid fuel spray on the main unstable pressure mode.
(a) Suppression of the "Lean" instability ($\phi = 0.4$); (b) Suppression of the "Rich" instability ($\phi = 1.1$).

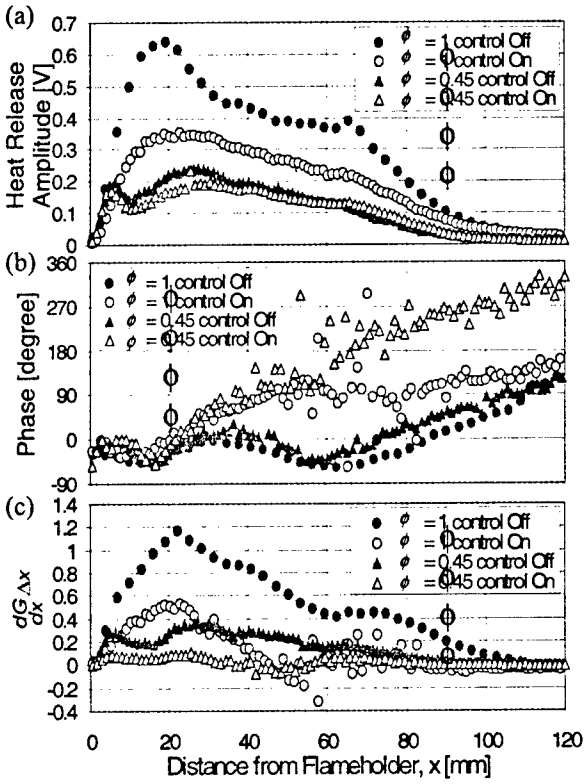

Figure 16. Effect of actively controlled modulation of liquid fuel spray on the oscillating flame characteristics.
(a) Heat release amplitude variation; (b) Phase angle variation; (c) Local Rayleigh index variation.